Int. J. Electrochem. Sci., 6 **(2011)** 4676 - 4689

International Journal of
ELECTROCHEMICAL
SCIENCE
www.electrochemsci.org

Catalytic Application of Gold Nanoparticles Electrodeposited by Fast Scan Cyclic Voltammetry to Glycerol Electrooxidation in Alkaline Electrolyte

Mohammad Etesami, Norita Mohamed[*]

School of Chemical Sciences, Universiti Sains Malaysia, 11800 USM, Penang, Malaysia
[*]E-mail: mnorita@usm.my

Received: 10 May 2011 / *Accepted:* 5 September 2011 / *Published:* 1 October 2011

A fast scan rate cyclic voltammetry was used to synthesis gold nanoparticles (AuNPs). AuNPs were electrodeposited on the surface of pencil graphite (PG) without using any additives in an acidic medium. The results depicted that the size of AuNPs varies by changing deposition time. The deposition time was changed by varying applied potential range, scan rate and number of cycles. PG and electrodeposited AuNPs were characterized by means of scanning electron microscopy (SEM), transmission electron microscopy (TEM) and X-ray diffraction (XRD). The results have shown that the smallest size of gold particles (20 ± 8 nm) was deposited on the PG substrate with almost spherical geometry at scan rate of 12500 mV s^{-1}. The electrocatalytic activity of AuNPs toward oxidation of glycerol was assessed in the alkaline medium by cyclic voltammetry. The effects of scan rate, temperature, potential limit, concentrations of glycerol and supporting electrolyte were studied by cyclic voltammetry. Moreover, the activity of AuNPs in long-term conditions was investigated with chronoamperometry.

Keywords: Gold nanoparticles, electrodeposition, electrooxidation of glycerol

1. INTRODUCTION

Direct alcohol fuel cells (DAFCs) have been studied as a portable source of energy that converts chemical energy to electrical energy. Amongst alcohols, methanol and ethanol are small organic molecules that have been investigated more often as a fuel in fuel cells. This is owing to their high energy production, ease of storage, handling and transportation of these fuels [1]. Alcohols like ethylene glycol (diol), glycerol (triol) and glucose (polyol) are of interest as fuel candidates for researchers due to their potential as liquid fuels [2-4]. Glycerol is one the most considerable compounds because of its versatile applications in the food and pharmaceutical industries [5, 6].

Glycerol, which can be generated from microbial fermentation, is a by-product in biodiesel production. Moreover, it is a promising alternative fuel in terms of safety, cost-effectiveness and environmental benefits. Glycerol is water-soluble and is less volatile and less toxic than ethanol and methanol [3, 7-9]. Also, in theory it can generate comparable mass energy density with other fuels (8.1, 6.1, 5.7, 5.2, 5 and 2.6 kWh kg^{-1} for ethanol, methanol, ammonia, ethylene glycol, glycerol and hydrazine) [10, 11]. Glycerol can be partially [12] or completely [13] oxidized at precious metal catalysts and can also produce various intermediates and species. The alkaline media are preferred to acidic electrolytes in fuel cells because they require less expensive catalysts, generate higher energy density and have faster kinetics of oxidation and reduction in both anode and cathode [14, 15]. The proposed mechanism for complete glycerol oxidation in alkaline media consists of releasing fourteen electrons [13].

Gold nanoparticles can be prepared using different chemical methods, such as direct electrodeposition, deposition–precipitation, sol–gel technique, impregnation, coprecipitation, metal organic-chemical vapor deposition, incipient wetness and dip-coating [16-21]. Their simple preparation, as well as their high surface area and variation in electronic and optoelectronic properties of nanosized materials, have made them more easily applicable than bulky substances. The superior catalytic behavior of gold was discovered by Haruta et al. when ultra-fine gold particles were synthesized via coprecipitation for the oxidation of carbon monoxide [22]. The importance of controlled shapes and sizes in gold deposit formation has been considered [23-26] because the performance of nanoparticles depends on their size and shape as well as the nature of their supporting materials [27, 28]. Gold has been electrodeposited in different conditions (the medium and gold solution concentration) and techniques [29-31]. Electrochemical deposition of gold nanoparticles (AuNPs) is a fast and convenient method of preparation [32, 33]. Synthesis of gold nanocrystals by electrodeposition was reported by applying a potential step to a glassy carbon electrode. The effects of applying different overpotentials and the concentration of gold deposition solutions on particle size were studied [34, 35]. Various sizes and geometries of gold nanocrystals have been formed via a potential step technique at different deposition times in both the presence and absence of additives (iodide and cysteine) [28, 36, 37]. Potential step electrolysis [38-41], pulse techniques [42, 43] and applying a constant potential [44, 45] are the voltammetric techniques for electrodeposition of AuNPs. AuNPs modified electrodes have been used in analysis[46-48] and catalysis [37, 39, 49].

In these experiments, gold nanoparticles were electrosynthesized by direct electrodeposition in an acidic medium via a fast scan cyclic voltammetry. The electrocatalytic application of gold nanoparticles was studied through electrooxidation of glycerol in alkaline electrolyte. Pencil graphite (PG) which has been used as a working electrode, is a cheap carbon-based material that has been utilized as a working electrode [50-54].

2.EXPERIMENTAL

2.1. Materials

$NaAuCl_4$. xH_2O (99.999 %), H_2SO_4 (97 %) and glycerol (99 %) were purchased from Sigma-Aldrich. Nitric acid, acetone, ethanol and NaOH were of analytical grade. All chemicals were used as

received. Flat PG lead (Unicorn Stationery Agency Sdn Bhd, Malaysia) was used as a working electrode (with an exposed geometrical area of 0.67 cm^2) in a three-electrode cell while Ag/AgCl (saturated KCl) and platinum wire were employed as reference and counter electrodes, respectively. The PG lead was treated each time before use by first being washed in acetone followed by being ultrasonically cleaned in ethanol and then distilled water for ten minutes each to remove any contamination. Distilled water (18 MΩ cm) was utilized during the work.

2.2. Instrumentation

Electrochemical experiments were carried out by an eDAQ EA 161 potentiostat connected to an e-corder 410 (4- channel recorder) equipped with EChem software v 2.1.0.

To characterize PG and AuNPs, a scanning electron microscope (SEM, Leo Supra 50 VP) equipped with an energy dispersive X-ray spectrometer (EDX) was used.

A PANalytical X'pert PRO MRD Pw 3040 X- ray diffractometer using Cu-Kα1 radiation (λ = 1.54056 Å) with a Ni filter working at 40 kV and 30 mA was used to collect X-ray diffraction (XRD) data. All samples were scanned from 5^o to 90^o (2θ).

The AuNPs were mechanically transferred to the surface of a copper grid for transmission electron microscope (TEM, Philips CM 12) analysis which was working at an accelerating voltage of 80 kV equipped with analysis software.

2.3. Electrodeposition of AuNPs on PG (AuNPs/PG)

The pretreated PG was immersed into deposition solutions of $NaAuCl_4$ (0.010, 0.10 and 1.0 mM), which were freshly prepared in 0.5 M H_2SO_4. Electrodeposition was carried out by applying varied ranges of potential, scan rates and number of cycles. All experiments (except for those investigating the effect of temperature on electrooxidation of glycerol) were performed at room temperature. All solutions were deaerated by bubbling nitrogen gas for ten minutes prior to each experiment. The N_2 gas was maintained over the solution during all experiments.

3. RESULTS AND DISCUSSION

3.1. The AuNPs/PG electrode

Fig. 1 is the cyclic voltammogram of $NaAuCl_4$ (1.0 mM) in 0.5 M H_2SO_4 solution at a PG electrode at a scan rate of 1000 mV s^{-1}. The anodic and cathodic peaks, a and c, are assigned to oxidation of gold and reduction of gold surface oxide, respectively. Peaks b and e are oxygen and hydrogen evolution while adsorption of protons occurs in region d [29, 30, 34]. The inset of Fig. 1 shows the potential shift of gold reduction peak at the first and second cycles. As seen, the peak in the second cycle has shifted to more positive potential which means easier electrodeposition of gold on the

existing gold particles. The quantity of gold electrodeposited on the PG electrode relies on deposition time.

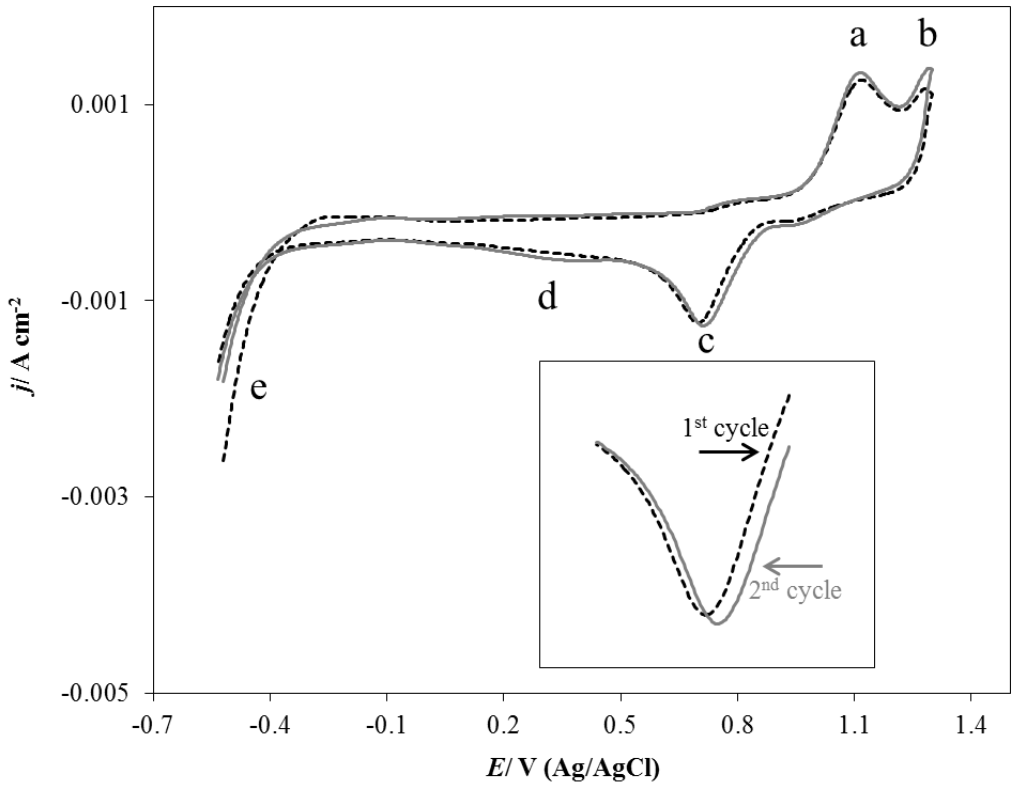

Figure 1. Cyclic voltammogram of $NaAuCl_4$ (1.0 mM) at PG electrode at a scan rate of 1000 mV s^{-1} in N_2- saturated 0.5 M H_2SO_4. Inset shows larger view of region c in the 1st and 2nd cycles.

Deposition time can be prolonged by performing more cycles, extending potential range or lowering scan rates. At extended deposition times and higher concentrations of gold solution, a golden color from the gold deposits can be observed. Similar to Gao et al. [37], during a prolonged deposition time, electrodeposited nanoparticles are not formed into spheres and in some parts aggregation of particles can be seen.

3.2. Characterization of AuNPs/PG electrode

The EDX analysis shows that the content of carbon in PG is more than 99% (Fig. 2). The inset shows the SEM micrograph of PG. To deposit AuNPs, the potential range (initial potential to 850 mV), in which the reduction of gold is the dominant reaction, is applied to the system. Fig. 3 shows the SEM images (3A and 3B) and TEM images (3C, 3D and 3E) for the electrodeposited AuNPs.

The SEM images (for bigger particles) and TEM images (for smaller particles) have been used for the calculating the average size of electrodeposited AuNPs. Table 1 shows the variation in average size of AuNPs versus the different applied conditions.

Table 1. The variation of average size of electrodeposited AuNPs with applied potential ranges, scan rates and number of cycles from different concentrations of $AuCl_4^-$ in N_2- saturated 0.5 M H_2SO_4.

Sample	Potential Range (mV)	Scan Rate (mV s^{-1})	[$AuCl_4^-$] (mM)	One cycle deposition time (ms)/ Total deposition time (s)	Average Size (nm)
1	0- 850	1000	1.0	1700/ 1700	81 ± 15
2	0- 850	5000	1.0	340/ 340	57 ± 13
3	0- 850	10000	1.0	170/ 170	32 ± 11
4	0- 850	12500	1.0	136/ 136	20 ± 8
5	0- 850	15000	1.0	113/ 113	43 ± 12
6	100- 850	12500	1.0	120/ 120	56 ± 10
7	−100- 850	12500	1.0	152/ 152	35 ± 9
8	0- 850	12500	0.10	136/ 136	14 ± 4.5
9	0- 850	12500	0.01	136/ 136	6 ± 1

Parameters that affect the deposition time are scan rate and number of cycles, which are applied to a specific range of potential. As can be seen from the results, at a lower scan rate (meaning a longer deposition time), particles have time to grow and aggregate. As shown in Fig. 3, in the potential range of 0 - 850 mV and for 1000 cycles and at an increased scan rate from 1000 mV s^{-1} to 15000 mV s^{-1}, AuNPs form different sizes. By performing in the aforementioned conditions, AuNPs with the average particle sizes of 81 ± 15, 57 ± 13, 32 ± 11, 20 ± 8 and 43 ± 12 nm are electrodeposited over the substrate at scan rates of 1000, 5000, 10000, 12500 and 15000 mV s^{-1}, respectively.

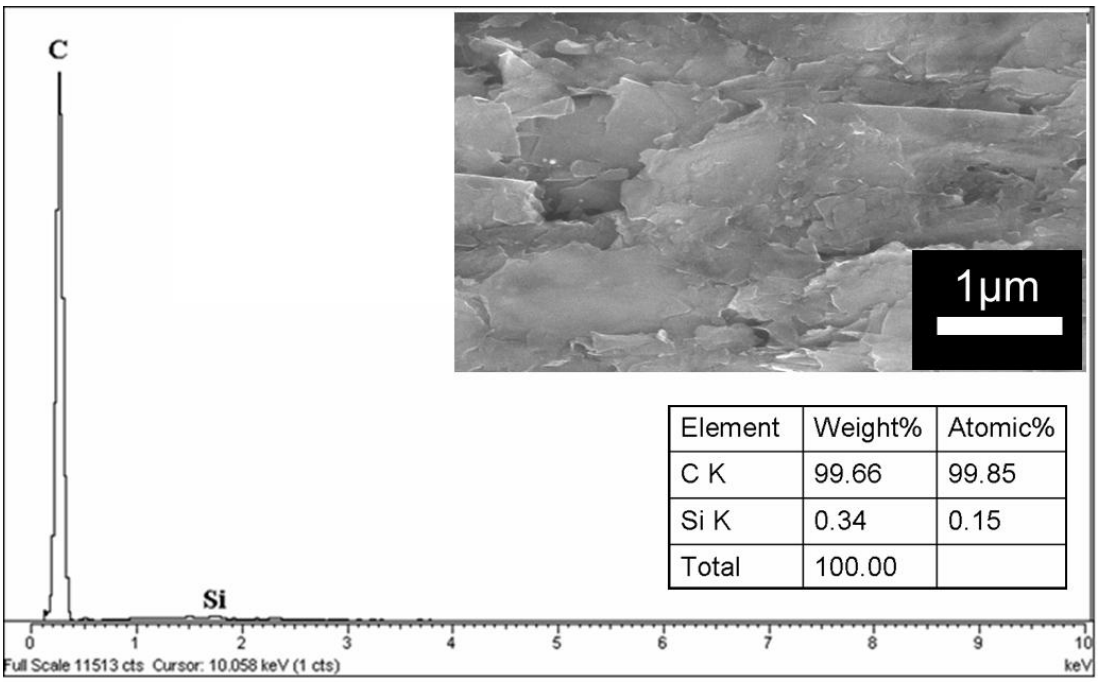

Figure 2. EDX and SEM micrograph (inset) of the surface area of the PG.

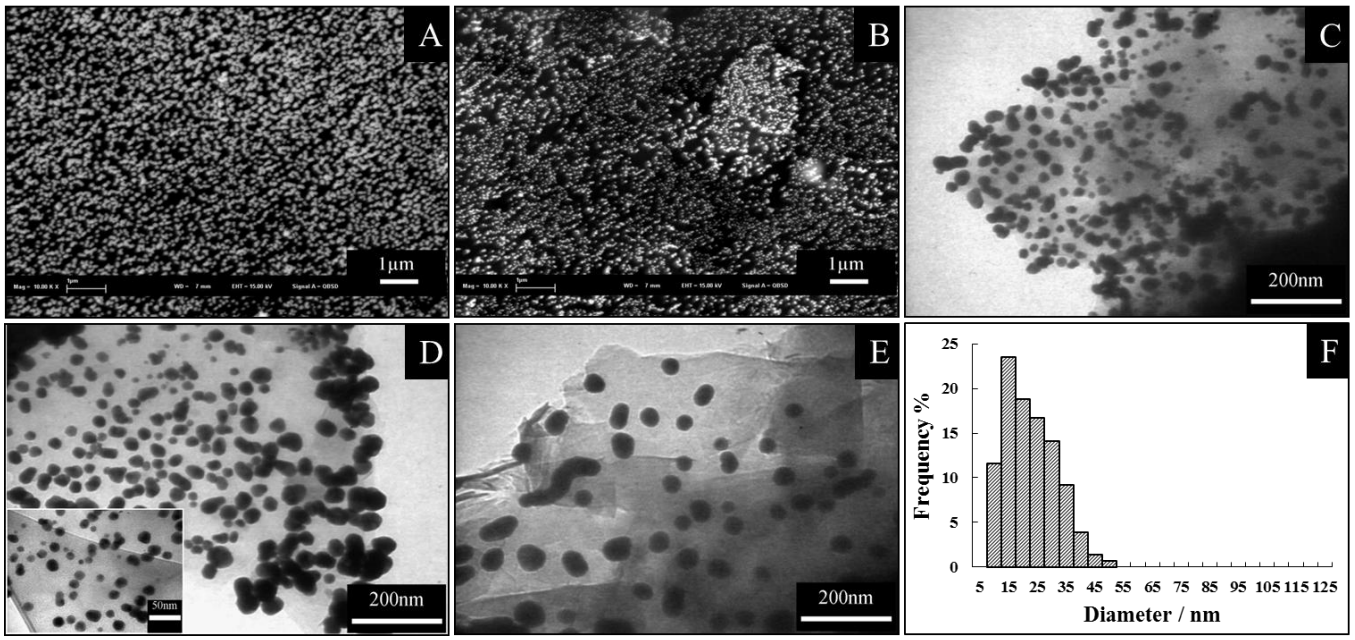

Figure 3. SEM micrographs (A and B) and TEM images (C, D and E) of AuNPs electrodeposited on the PG electrode from N_2- saturated 0.5 M H_2SO_4 solution containing 1.0 mM $NaAuCl_4$. Applied conditions (potential range/ scan rate/ number of cycles) are (A) 0 - 850/ 1000/ 1000 (sample 1), (B) 0 - 850/ 5000/ 1000 (sample 2), (C) 0 - 850/ 10000/ 1000 (sample 3), (D) 0 - 850/ 12500/ 1000 (sample 4) and (E) 0 - 850/ 15000/ 1000 (sample 5). Histogram of the electrodeposited Au nanoparticle size distribution of sample 4 (F).

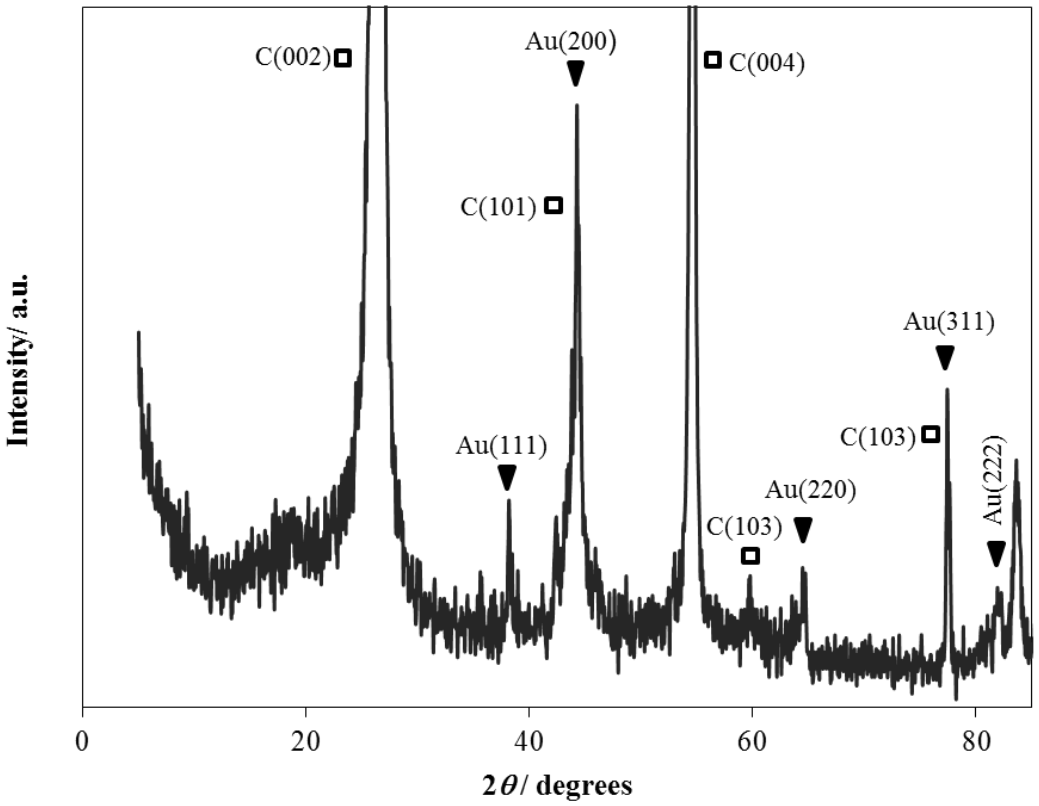

Figure 4. XRD diffraction pattern of sample 4.

The deposition of nanoparticles includes two main processes: first, fast nucleation, followed by growth. To reach a definite size of electrodeposited nanoparticles, nucleation and growth should be controlled. Initial potential is an important parameter in cyclic voltammetry. Different initial potentials were applied to samples 4 (0 mV), 6 (100 mV) and 7 (-100 mV), forming various average sizes of AuNPs (Table 1). The smallest average size of electrodeposited AuNPs was obtained with sample 4 (the histogram is shown in Fig. 3F). According to results, the optimum condition for nucleation and growth was attained with an initial potential of 0 mV. It is assumed that the initial applied potential of 100 mV (sample 6) is not sufficient to reach the desired level of nucleation on the surface of the electrode but is adequate for particle growth [55]. Prolonged deposition time resulted in a longer growth process with sample 7, which caused larger particle aggregation in some parts.

From the XRD data (Fig. 4) obtained from AuNPs/PG samples, PG shows a hexagonal crystalline structure with C(002), C(004), C(100), C(101), C(103) and C(110) facets while all samples of AuNPs have Face-Centered Cubic (FCC) crystal structure with Au(111), (200), (220), (311) and (222) facets.

3.3. Electrooxidation of glycerol on AuNPs/PG

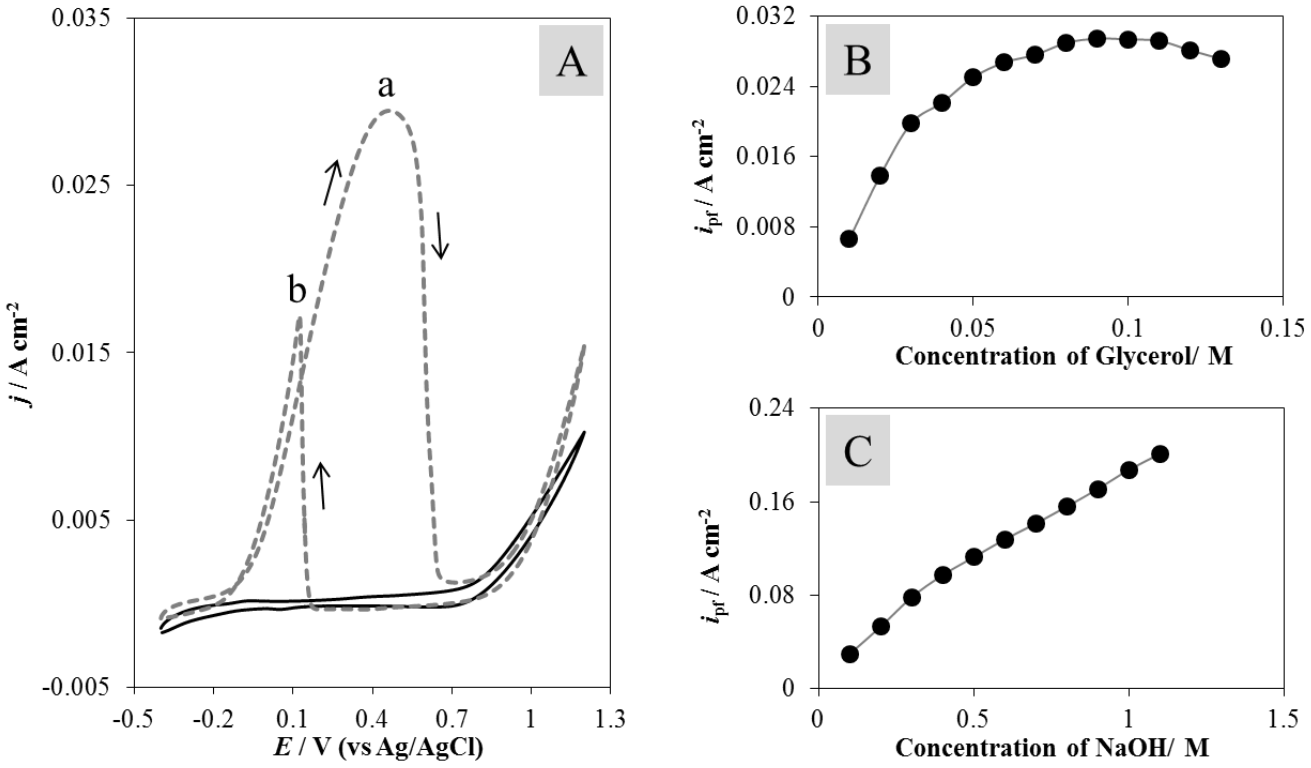

Figure 5. Cyclic voltammograms of AuNPs/PG in 0.1 M NaOH (——) and containing 0.09 M glycerol (– –) at scan rate of 100 mV s^{-1} (A). Variation of forward anodic peak current for electrooxidation of glycerol versus concentration of (B) glycerol in 0.1 M NaOH and (C) NaOH in 0.09 M glycerol on the AuNPs/PG at scan rate of 100 mV s^{-1}.

Electrodeposited AuNPs with an average diameter of 20 ± 8 nm have been used in the electrooxidation of glycerol.

A cyclic voltammogram of AuNPs/PG in 0.1 M NaOH containing 0.09 M glycerol is shown in Fig. 5A. The cyclic voltammograms show that activity of AuNPs/PG electrode in the 0.1 M NaOH is negligible. According to Jeffery and Camara [1], theoretically, complete oxidation of glycerol in alkaline media is as follows:

$$CH_2OH - CHOH - CH_2OH + 20\ OH^- \rightarrow 3CO_3^{2-} + 14H_2O + 14\bar{e} \quad (1)$$

The anodic peak a in the positive-going (forward) scan is attributed to electrooxidation of glycerol to its intermediates and the anodic peak b in the negative-going (backward) scan is ascribed to oxidation of intermediate species or residues, which remained in the solution from the forward scan. The heights of forward (i_{pf}) and backward (i_{pb}) anodic peak currents depend on parameters such as temperature, scan rate, the amount of metal nanoparticles loaded on the surface of electrode, as well as the concentration of supporting electrolyte and (for i_{pb}) species formed on the surface of metal nanoparticles [56, 57].

3.3.1. Effect of concentrations

The concentrations of oxidant and supporting electrolytes affect the activity of AuNPs towards electrooxidation process [58].

To evaluate the capacity of AuNPs for electrooxidation of glycerol, different concentrations of glycerol were surveyed with a constant concentration of the supporting electrolyte by cyclic voltammetry.

It can be seen in Fig. 5B that the capacity of AuNPs for electrooxidation of glycerol increases with glycerol concentration up to 0.09 M glycerol. i_{pf} reaches a near-constant value and then decreases slightly. The active sites at the surface of AuNPs might be fully saturated at a concentration of 0.09 M glycerol.

The effect of varying concentrations of NaOH on the anodic peak current of glycerol at a scan rate of 100 mV s^{-1} was studied by cyclic voltammetry. The variation of i_{pf} related to glycerol oxidation versus the concentration of NaOH is depicted in Fig. 5C.

The anodic current increases with higher concentrations of NaOH. According to the proposed mechanism, electrooxidation of glycerol is thermodynamically favored in an alkaline medium [10, 59, 60].

3.3.2. Effect of scan rate

The effect of scan rate on the electrooxidation of 0.09 M glycerol in 0.1 M NaOH by cyclic voltammetry is shown in Fig. 6A. Fig. 6B represents the variation of i_{pf} versus the square root of the scan rate.

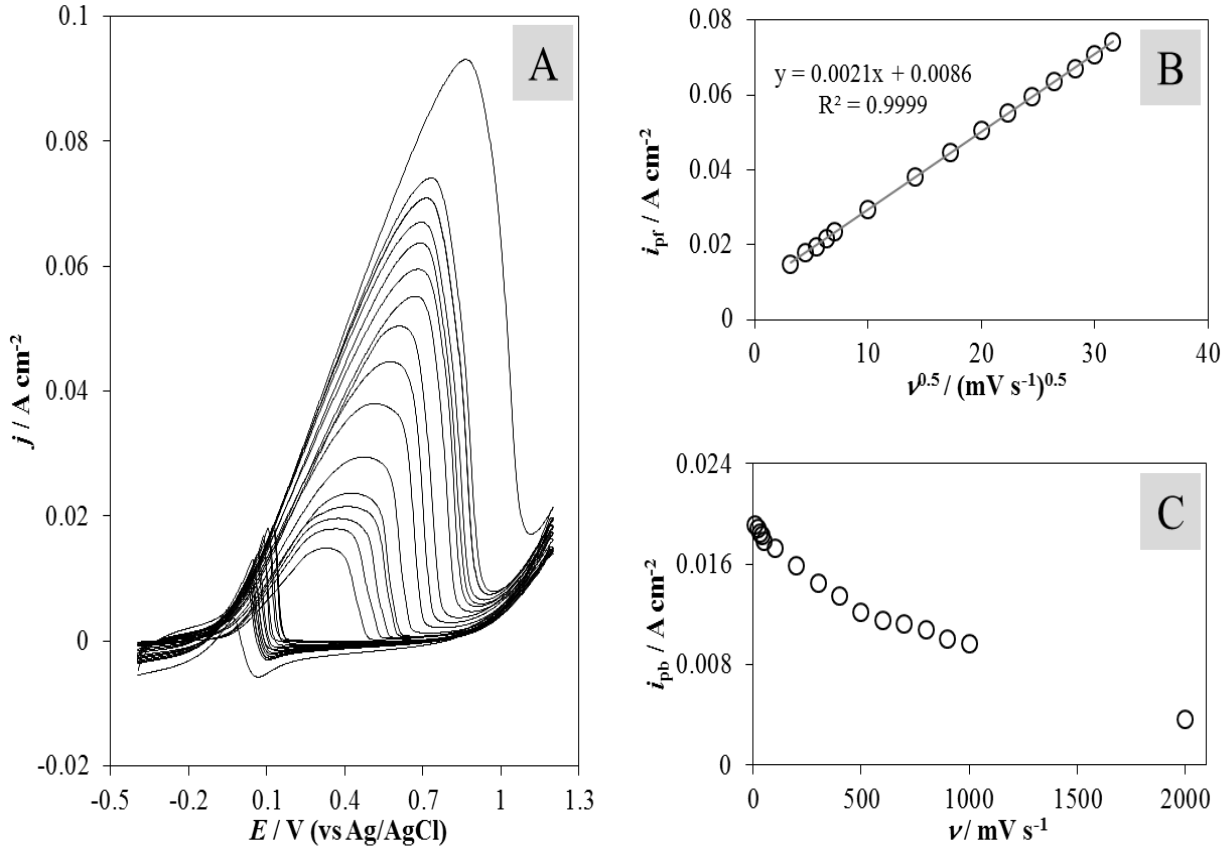

Figure 6. Cyclic voltammetric responses of AuNPs/PG in 0.1 M NaOH containing 0.09 M glycerol at different scan rates: (from inner to outer cycle) 10, 20, 30, 40, 50, 100, 200, 300, 400, 500, 600, 700, 800, 900, 1000 and 2000 mV s^{-1} (A). The variation of anodic peak current in forward (i_{pf}) versus square root of scan rate from scan rate of 10- 1000 mV s^{-1} (B) and the variation of anodic peak current in backward (i_{pb}) versus scan rate (C).

The anodic peak current in the forward scan (i_{pf}) increases proportionally with the increasing scan rate while the anodic peak current in the backward scan (i_{pb}) decreases proportionally with the increasing scan rate. It can be concluded that at lower scan rates the species produced from the forward scan have had enough time to be adsorbed on the surface of AuNPs. Thus, the related i_{pb} shows higher magnitudes at lower scan rates (Fig. 6C). Despite the linear curve ($r^2 = 0.9999$) for i_{pf} versus $\square^{0.5}$, the electrooxidation of glycerol on the surface of AuNPs is not a fully diffusion-controlled process because of the non-zero intercept of the equation.

3.3.3. Effect of potential limit

Fig. 7A. shows the cyclic voltammograms of AuNPs/PG in 0.09 M glycerol + 0.1 M NaOH at a scan rate of 100 mV s^{-1} with different final potentials. As can be seen, the i_{pf} remained constant while the i_{pb} decreased and their relative potentials shifted to negative potentials. It is assumed that with a more positive final potential, more gold oxide is produced [61] and the association of residual species generated from the forward scan decreases on the surface of catalyst [9].

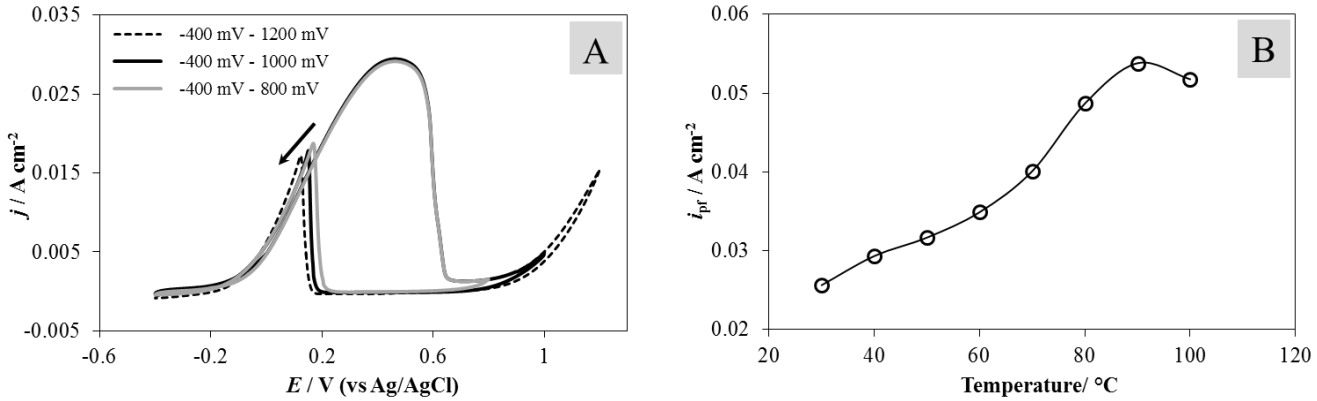

Figure 7. Cyclic voltammograms of AuNPs/PG in 0.1 M NaOH containing 0.09 M glycerol at different final potentials (A). The variation of anodic peak current in forward scan (i_{pf}) at different medium temperature (B).

3.3.4. Effect of temperature

Cyclic voltammograms of AuNPs/PG in 0.09 M glycerol + 0.1 M NaOH that were exposed to different solution temperature are presented in Fig. 7B. The cyclic voltammograms of 0.09 M glycerol + 0.1 M NaOH were carried out at intervals of 10℃ starting from 30℃. The anodic peak currents (in forward and reverse sweep) increase with increasing temperature up to 90℃, which indicates acceleration of electrooxidation of glycerol on the AuNPs at a higher temperature. At temperatures near 100℃, water molecules evaporate and deviate from the diffusion control process (agitation of solution), so the aforementioned trend was not followed. It is assumed that the electrooxidation of glycerol is a temperature-dependent process since, the anodic current peaks (i_{pf} and i_{pb}) increase to higher values and the inset potential shifts to more negative potentials. As reported earlier [62], the adsorption of polyols on the surface of gold increases with higher temperatures because of the partial loss of water molecules from the hydration shell around the surface of the gold and polyol.

3.3.5. Chronoamperometry

To study the oxidation performance of AuNPs under long-term conditions, chronoamperometric experiments were carried out. Fig. 8. shows choronoamperograms of AuNPs at potentials of 0, 100, 200, 300 and 400 mV in 0.09 M glycerol + 0.1 M NaOH for 120s.

As shown, the current density decreases quickly at first because of the poisoning of AuNPs by generated species before reaching a stable value. The largest current density can be seen in 400 mV, which is in agreement with the cyclic voltammogram in Fig. 5.

3.3.6. Long-term stability of AuNPs/PG electrode

The behavior of the AuNPs/PG electrode in 0.09 M glycerol + 0.1 M NaOH in a successive number of cycles has also been investigated. The current density of the anodic peak in the forward scan (i_{pf}) versus number of cycles is shown in Fig. 9.

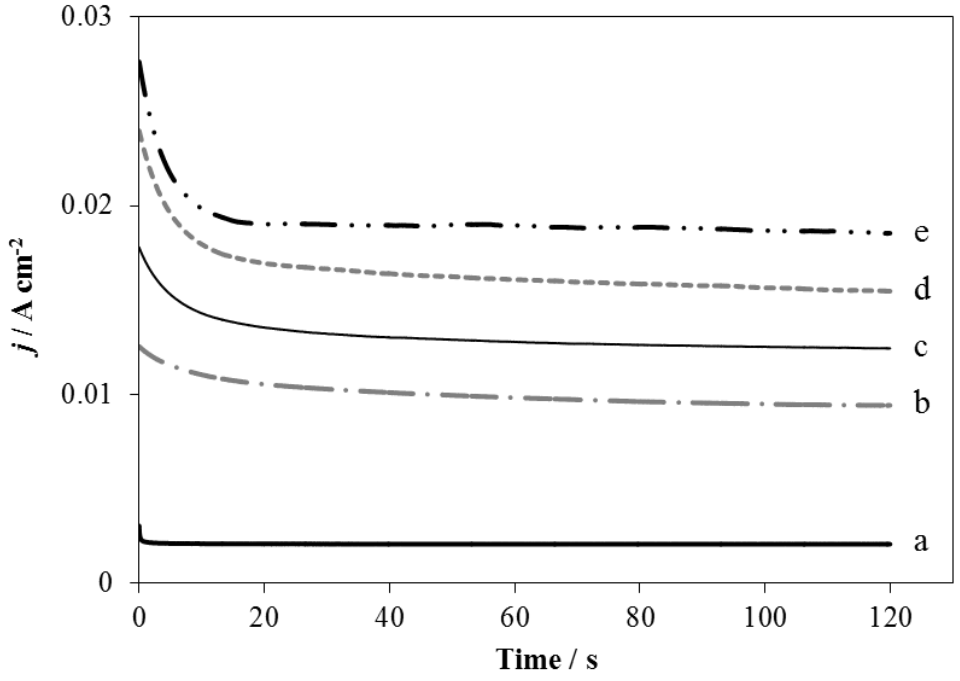

Figure 8. Chronoamperometric curves of AuNPs/PG in 0.1 M NaOH + 0.09 M glycerol at constant potential of (a) 0 mV, (b) 100 mV, (c) 200 mV, (d) 300 mV and (e) 400 mV for 120 s.

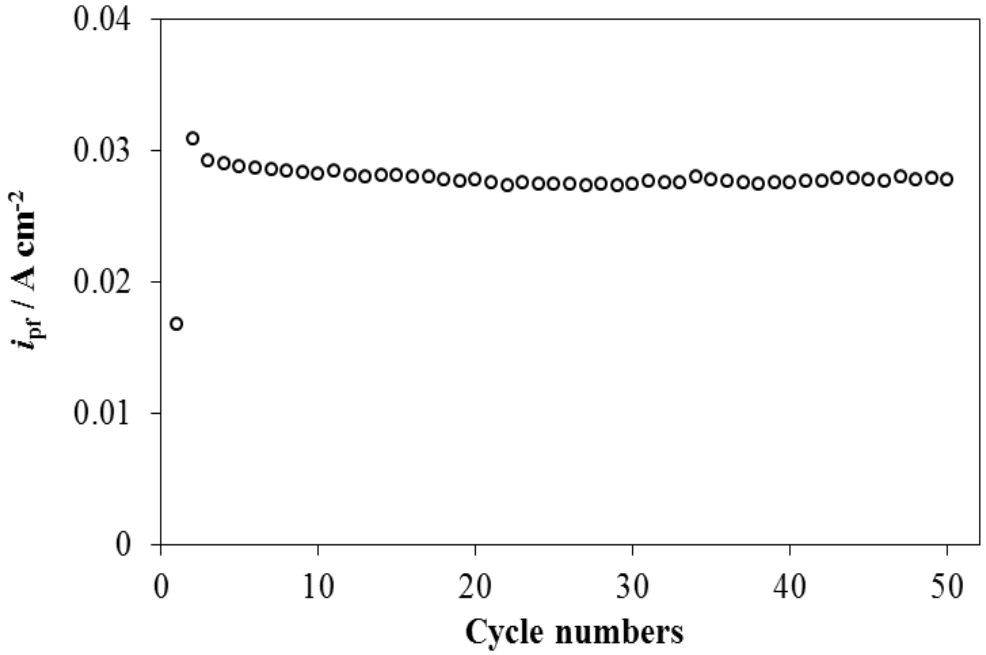

Figure 9. The variation of anodic current density in forward scan (i_{pf}) in fifty successive scan cycles.

To study the long-term stability of the AuNPs/PG electrode, fifty successive cycles were applied to the working electrode in the potential range of -400 mV to 1200 mV at scan rate of 100 mV s^{-1}. The data show after a decrease in the first cycle, the anodic current density remains constant. It is supposed that the incomplete adsorption of glycerol molecules on the surface of AuNPs causes weaker

anodic current density in the first cycle. The anodic current density of the 200th cycle is about 90% that of the third cycle which is due to the effect of poisonous species on the AuNPs. After continuous usage for 5 months, the average of current density showed about 3% decrease in comparison with the prepared AuNPs/PG electrode.

4. CONCLUSIONS

Various sizes of AuNPs were deposited on the PG electrode via fast scan cyclic voltammetry by varying the applied parameters (e.g. scan rate, applied deposition time and number of cycles). By using this technique without any additives, AuNPs were electrodeposited on the surface of pencil graphite. TEM images illustrated that the smallest average particle size of electrodeposited AuNPs achieved, was 20 ± 8 nm when a scan rate of 12500 mV s^{-1} in a potential range of 0- 850 mV and with 1000 cycles was applied. The catalytic property of synthesized AuNPs was investigated by studying the electrooxidation of glycerol. The optimized concentration achieved for glycerol was 0.09 M in 0.1 M NaOH while the anodic current increased at higher concentrations of supporting electrolyte. As the scan rate increases, the anodic peaks in the forward and backward scan vary. From the equation and linear curve obtained from i_{pf} versus square root of scan rate, it was observed that the electrooxidation of glycerol on the AuNPs/PG is not fully controlled by a diffusion process. The effect of temperature and potential limit were also investigated by cyclic voltammetry. Chronoamperometric experiments confirmed that the AuNPs/PG electrode was poisoned by generated intermediates. Finally, the AuNPs/PG electrode showed stability after 5 months of use.

ACKNOWLEDGMENTS
This research has been supported by a RU-Grant (1001/ PKIMIA/ 811056) from Universiti Sains Malaysia (USM). M. Etesami would like to thank USM for a fellowship scheme.

References

1. D. Z. Jeffery and G. A. Camara, *Electrochem. Commun.*, 12 (2010) 1129
2. Y. Choi, G. Wang, M. H. Nayfeh and S.-T. Yau, *Biosens. Bioelectron.*, 24 (2009) 3103
3. A.Nirmala Grace and K. Pandian, *Electrochem. Commun.*, 8 (2006) 1340
4. W. M. Nobanathi , I. O. Kenneth and J. A. Christopher *Electroanalysis*, 22 (2010) 519
5. K. Saito, A. M. Ahhmed, S. Kawahara, Y. Sugimoto, T. Aoki and M. Muguruma, *Food. Sci. Technol. Res*, 15 (2009) 283
6. N. Atrux-Tallau, C. Romagny, K. Padois, A. Denis, M. Haftek, F. Falson, F. Pirot and H. Maibach, *Arch. Dermatol. Res.*, 302 (2010) 435
7. L. M. Lourenço and N. R. Stradiotto, *Talanta*, 79 (2009) 92
8. I.-S. Park, K.-S. Lee, S. J. Yoo, Y.-H. Cho and Y.-E. Sung, *Electrochim. Acta*, 55 (2010) 4339
9. L. Su, W. Jia, A. Schempf and Y. Lei, *Electrochem. Commun.*, 11 (2009) 2199
10. M. Simões, S. Baranton and C. Coutanceau, *Appl. Catal., B- Environ*, 93 (2010) 354
11. F. Vigier, C. Coutanceau, A. Perrard, E. M. Belgsir and C. Lamy, *J. Appl. Electrochem.*, 34 (2004) 439

12. G. Yildiz and F. Kadirgan, *J. Electrochem. Soc.*, 141 (1994) 725
13. R. L. Arechederra and S. D. Minteer, *Fuel Cells*, 9 (2009) 63
14. E. H. Yu, U. Krewer and K. Scott, *Energies*, 3 (2010) 1499
15. E. Antolini and E. R. Gonzalez, *J. Power Sources*, 195 (2010) 3431
16. Y. Ma, J. Di, X. Yan, M. Zhao, Z. Lu and Y. Tu, *Biosens. Bioelectron.*, 24 (2009) 1480
17. F. El-Cheick, F. Rashwan, H. Mahmoud and M. El-Rouby, *J. Solid State Electrochem.*, 14 (2010) 1425
18. S. Schimpf, M. Lucas, C. Mohr, U. Rodemerck, A. Brückner, J. Radnik, H. Hofmeister and P. Claus, *Catal. Today*, 72 (2002) 63
19. H. Berndt, A. Martin, I. Pitsch, U. Prüsse and K. D. Vorlop, *Catal. Today*, 91-92 (2004) 191
20. D. B. Akolekar and S. K. Bhargava, *J. Mol. Catal. A: Chem.*, 236 (2005) 77
21. H. Shi, H. Bi, B. Yao and L. Zhang, *Appl. Surf. Sci.*, 161 (2000) 276
22. M. Haruta, T. Kobayashi, H. Sano and N. Yamada, *Chem. Lett.* (1987) 405
23. L. Wang, S. Guo, X. Hu and S. Dong, *Electrochem. Commun.*, 10 (2008) 95
24. H.-X. Ren, X.-J. Huang, O. Yarimaga, Y.-K. Choi and N. Gu, *J. Colloid Interface Sci.*, 334 (2009) 103
25. G. Kawamura and M. Nogami, *J. Cryst. Growth*, 311 (2009) 4462
26. S. Y. Moon, T. Kusunose and T. Sekino, *Mater. Lett.*, 63 (2009) 2038
27. C. Welch and R. Compton, *Anal. Bioanal. Chem.*, 384 (2006) 601
28. M. S. El-Deab, *Electrochim. Acta*, 54 (2009) 3720
29. G. Trejo, A. F. Gil and I. Gonzalez, *J. Electrochem. Soc.*, 142 (1995) 3404
30. U. Schmidt, M. Donten and J. G. Osteryoung, *J. Electrochem. Soc.*, 144 (1997) 2013
31. X. Wang, N. Isaev and J. G. Osteryoung, *J. Electrochem. Soc.*, 143 (1996) 1201
32. Y. Zhang, S. Asahina, S. Yoshihara and T. Shirakashi, *Electrochim. Acta*, 48 (2003) 741
33. M. S. El-Deab, T. Sotomura and T. Ohsaka, *J. Electrochem. Soc.*, 152 (2005) C1
34. M. O. Finot, G. D. Braybrook and M. T. McDermott, *J. Electroanal. Chem.*, 466 (1999) 234
35. M. O. Finot and M. T. McDermott, *J. Electroanal. Chem.*, 488 (2000) 125
36. M. S. El-Deab, T. Sotomura and T. Ohsaka, *J. Electrochem. Soc.*, 152 (2005) C730
37. F. Gao, M. S. El-Deab, T. Okajima and T. Ohsaka, *J. Electrochem. Soc.*, 152 (2005) A1226
38. X. Dai and R. G. Compton, *Electroanalysis*, 17 (2005) 1325
39. M. S. El-Deab, T. Sotomura and T. Ohsaka, *Electrochim. Acta*, 52 (2006) 1792
40. M. S. El-Deab, T. Sotomura and T. Ohsaka, *Electrochem. Commun.*, 7 (2005) 29
41. X. Dai, O. Nekrassova, M. E. Hyde and R. G. Compton, *Anal. Chem.*, 76 (2004) 5924
42. H. Liu and R. M. Penner, *J. Phys. Chem. B*, 104 (2000) 9131
43. R. M. Penner, *J. Phys. Chem. B*, 106 (2002) 3339
44. P. Norouzi, B. Larijani, F. Faridbod and M. R. Ganjali, *Int. J. Electrochem. Sci.*, 5 (2010) 1550
45. K. A. Mahmoud, S. Hrapovic and J. H. T. Luong, *ACS Nano*, 2 (2008) 1051
46. M. Behpour, S. M. Ghoreishi and E. Honarmand, *Int. J. Electrochem. Sci.*, 5 (2010) 1922
47. T. Ndlovu, O. A. Arotiba, R. W. Krause and B. B. Mamba, *Int. J. Electrochem. Sci.*, 5 (2010) 1179
48. F. W. Campbell and R. G. Compton, *Anal. Bioanal. Chem.*, 396 (2010) 241
49. M. S. El-Deab and T. Ohsaka, *J. Electroanal. Chem.*, 553 (2003) 107
50. I.M. Isa and S. Ab Ghani, *Food Chem.*, 112 (2009) 756
51. A.Doménech, M. T. Doménech-Carbó and I. Martínez-Lázaro, *Anal. Chim. Acta*, 680 (2010) 1
52. U. Chandra, B. E. Kumara Swamy, O. Gilbert, M. Pandurangachar, S. Reddy, S. S. Shankar and B. S. Sherigara, *Chin. Chem. Lett.*, 21 (2010) 1490
53. M. Sönmez, M. Çelebi, Y. YardIm and Z. Sentürk, *Eur. J. Med. Chem.*, 45 (2010) 4215
54. A.Levent, Y. Yardim and Z. Senturk, *Electrochim. Acta*, 55 (2009) 190
55. Y. Wang, J. Deng, J. Di and Y. Tu, *Electrochem. Commun.*, 11 (2009) 1034
56. H. Razmi, E. Habibi and H. Heidari, *Electrochim. Acta*, 53 (2008) 8178

57. N. G. Ahmad, G. M. Mohammad, S. S. Sajjad, M. T.-G. Karim and Y. Mohammad, *Electroanalysis*, 18 (2006) 911
58. R. S. Ferreira Jr, V. R. Oliveira, R. G. C. S. Reis, G. Maia and G. A. Camara, *J. Power Sources*, 185 (2008) 853
59. A.T. Marshall and R. G. Haverkamp, *Int. J. Hydrog. Energy*, 33 (2008) 4649
60. M. L. Avramov-Ivic, J. M. Leger, C. Lamy, V. D. Jovic and S. D. Petrovic, *J. Electroanal. Chem.*, 308 (1991) 309
61. B. Guo, S. Zhao, G. Han and L. Zhang, *Electrochim. Acta*, 53 (2008) 5174
62. O. Enea and J. P. Ango, *Electrochim. Acta*, 34 (1989) 391